tion of the maximum heat transport rate; however, this finding was inconclusive. Although this conclusion can be strictly applied only to this pipe at the vibration frequencies and levels tested, it can be expected to be applicable to pipes of similar construction at levels of vibration near to those evaluated here.

References

[1]Deverall, J. E., "The Effect of Vibration on Heat Pipe Performance," Los Alamos Scientific Laboratory, Los Alamos, NM LA-3798, Oct. 1967.

[2]Richardson, J. W. et al., "The Effect of Longitudinal Vibration on Heat Pipe Performance," *Journal of Astronautical Sciences*, Vol. 17, No. 5, 1970, pp. 249–265.

[3]Charlton, M. C., and Bowman, W. J., "Effect of Transverse Vibration on the Capillary Limit of a Wrapped Screen Wick Copper/Water Heat Pipe," AIAA Paper No. 93–2734, July 1993.

Dynamical Instability of the Aerogravity Assist Maneuver

Colin R. McInnes*
University of Glasgow,
Glasgow G12 8QQ, Scotland, United Kingdom

Introduction

THE use of aerodynamic lift for the modification of conventional gravity-assist trajectories has recently been discussed as a means of enabling certain inner and outer solar-system missions.[1,2] Using a high-lift-to-drag vehicle, such as the waverider type,[3] trajectory bending angles far in excess of what may be obtained using ballistic gravity assist alone are attainable.

The aerogravity-assist (AGA) trajectory is essentially an equilibrium solution to the dynamical equations. With the vehicle in an inverted configuration, aerodynamic lift and the gravitational acceleration balance the normal acceleration due to trajectory curvature.

In this study the fundamental dynamical equations are used to form a single expression for the vertical acceleration. It is then demonstrated that for initial errors in altitude the resulting AGA trajectory is exponentially unstable. This may lead to the vehicle prematurely exiting the planetary atmosphere or impacting on the surface in some instances. It is however demonstrated that feedback linearization may be used to ensure stability and tracking of the required altitude for equilibrium flight.

Although there are many dynamical issues associated with the AGA maneuvre (e.g., atmospheric uncertainties), this analysis highlights the need for precise guidance, navigation, and control to ensure a successful atmospheric pass meeting the required exit conditions.

AGA Flight Dynamics

For ease of illustration the dynamical equations are formulated in a nonrotating wind-free atmosphere. The vehicle position is described by planetocentric polar coordinates (r, θ), and the vehicle motion is described by the inertial velocity v and flight-path angle γ, as shown in Fig. 1. In this analysis the vehicle uses the bank angle σ as a single control input for lift modulation, with the angle of attack trimmed for maximum lift. The two dynamical and two kinematic equations are therefore given by

$$\frac{dv}{dt} = -\frac{D}{m} + g\sin\gamma \tag{1a}$$

$$v\frac{d\gamma}{dt} = -\left(\frac{v^2}{r} - g\right)\cos\gamma - \frac{L}{m}\cos\sigma \tag{1b}$$

Received Oct. 10, 1992; revision received Dec. 15, 1992; accepted for publication Dec. 16, 1992.

*Department of Aerospace Engineering.

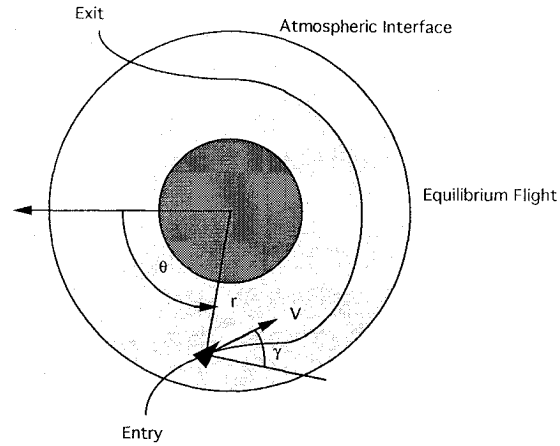

Fig. 1 Schematic geometry of the aerogravity assist maneuver.

$$\frac{dr}{dt} = -v\sin\gamma \tag{1c}$$

$$\frac{d\theta}{dt} = \frac{v}{r}\cos\gamma \tag{1d}$$

where g is the planetary gravitational acceleration. The aerodynamic lift and drag are defined in terms of the lift and drag coefficients C_L and C_D as

$$\begin{Bmatrix} L \\ D \end{Bmatrix} = \tfrac{1}{2}\rho(r)Sv^2\begin{Bmatrix} C_L \\ C_D \end{Bmatrix} \tag{2}$$

where S is the aerodynamic reference area and the atmospheric density ρ is assumed to be a function of altitude only.

Differentiating Eq. (1c) and substituting, an expression for the vertical acceleration may be derived as

$$\frac{d^2r}{dt^2} = \frac{v^2}{r}\cos^2\gamma - g + \frac{D}{m}\sin\gamma + \frac{L}{m}\cos\sigma\cos\gamma \tag{3}$$

For the AGA maneuver level, constant-altitude flight is required so that the left-hand side of Eq. (3) vanishes. Setting $\gamma = 0$, the required bank angle σ^* may then be obtained as

$$\sigma^* = \cos^{-1}\left[\frac{2m}{\rho(r)C_LS}\left(\frac{g}{v^2} - \frac{1}{r}\right)\right] \tag{4}$$

where $\pi/2 < \sigma^* < 3\pi/2$, as the vehicle must be oriented in an inverted configuration with the aerodynamic lift and gravity in equilibrium with the outward normal acceleration. Transverse motion may be eliminated by periodic roll reversals, unless there is a specific requirement for a plane change.

For the cases of interest with atmospheric entry at large hyperbolic velocities, the gravitational acceleration may be neglected with respect to the aerodynamic and normal accelerations. The required bank angle is then a function of altitude only.

Linear Stability Analysis

In order to investigate the stability of the AGA maneuver the vertical acceleration equation will be perturbed with the vehicle initial flight-path angle $\gamma_0 = 0$ and velocity v_0 fixed. Perturbing the vehicle altitude so that $r \to r_0 + \xi$ in Eq. (3) and retaining terms of order ξ, it is found that

$$\frac{d^2\xi}{dt^2} + \left[\frac{v^2}{r^2} + \frac{\rho'(r)}{\rho(r)}\left(\frac{v^2}{r} - g(r)\right) + g'(r)\right]_0\xi + O(\xi^2) = 0 \tag{5}$$

where the required bank angle σ^* has been substituted from Eq. (4). This variational equation is of the standard form with solution $\xi(t)$, viz.,

$$\frac{d^2\xi}{dt^2} + \Lambda^2(v_0, r_0)\xi = 0 \to \xi(t) = \xi_{01}e^{-\sqrt{\Lambda^2}t} + \xi_{02}e^{-\sqrt{\Lambda^2}t} \tag{6}$$

It should be noted that the vehicle velocity v is here fixed, whereas in fact it is slowly decreasing due to drag losses, leading to a slowly time-varying coefficient in Eq. (6).

For a stable, bounded solution in Eq. (6) it is required that $\Lambda^2 > 0$, a condition which may be written as

$$v < \sqrt{g(r)r}\left(\frac{\frac{\rho'(r)}{\rho(r)} - \frac{g'(r)}{g(r)}}{\frac{1}{r} + \frac{\rho'(r)}{\rho(r)}}\right)^{\frac{1}{2}} \tag{7}$$

where $[g(r)r]^{\frac{1}{2}}$ is the Keplerian circular velocity at altitude r. The inequality in Eq. (7) may be evaluated for any spherically symmetric atmosphere and gravity model. However, for the usual inverse-square gravitational acceleration and exponential atmosphere it is found that

$$\frac{\rho'(r)}{\rho(r)} = -\frac{1}{H} \tag{8a}$$

$$\frac{g'(r)}{g(r)} = -\frac{2}{r} \tag{8b}$$

where H is the scale height in the atmosphere, which in general is a function of altitude.

With a constant atmospheric scale height the stability condition may be written as

$$v < \sqrt{g(r)r}\left(\frac{r/H - 2}{r/H - 1}\right)^{\frac{1}{2}} \tag{9}$$

For typical planetary atmospheres $r/H \gg 1$, so that for stability it is required that $v < [g(r)r]^{\frac{1}{2}}$ (i.e., the vehicle must have a velocity less than or equal to the local Keplerian orbital velocity). For all AGA maneuvers the entry and exit velocities will be hyperbolic, so that the stability condition defined by Eq. (9) is never met. It is therefore concluded that all AGA-type maneuvres are in fact dynamically unstable.

This instability may be readily understood physically, as the AGA maneuver is an equilibrium path with aerodynamic lift and gravity balancing the normal acceleration. Neglecting gravity for the moment, it is clear that as the vehicle altitude increases, the inward aerodynamic lift falls exponentially, whereas the normal acceleration falls only inversely as the altitude, resulting in a net outwards, destabilizing acceleration.

The time scale of the instability, τ, may be estimated from $\Lambda(v, r)$ in terms of the equivalent time to complete a single orbit at hyperbolic velocity $T = 2\pi r/v$:

$$\tau = T\left[\left(\frac{r}{H} - 1\right) - \frac{g(r)r}{v^2}\left(\frac{r}{H} - 2\right)\right]^{-\frac{1}{2}} \tag{10}$$

Neglecting the gravitational acceleration, the instability time scale may be written simply as $\tau = T(r/H)^{-\frac{1}{2}}$.

Feedback Linearization Guidance

Now that the AGA instability has been demonstrated, a nonlinear transformation technique will be applied to ensure stability and tracking of the required altitude. This technique has been successfully applied to the guidance of air-breathing aerospace vehicles.[4] In this case the vehicle bank angle will be used to control the vertical component of the aerodynamic lift. Since it is required to track an altitude of r_0, successive derivatives of r are taken until the control appears explicitly; cf. Eq. (3). The bank angle appears in the second derivative of r, and so a pseudocontrol U is defined as

$$U \equiv \frac{\mathrm{d}^2 r}{\mathrm{d}t^2} \tag{11}$$

Then, to ensure stability, the pseudocontrol is defined by the altitude error and error rate as

$$U = \lambda_1(r_0 - r) - \lambda_2\frac{\mathrm{d}r}{\mathrm{d}t} \tag{12}$$

where the feedback gains λ_1 and λ_2 are chosen to achieve the desired response of the vehicle about the nominal equilibrium path. Inverting Eq. (3), the required bank angle is obtained as

$$\cos\sigma = \frac{m}{L\cos\gamma}\left[\left(\frac{v^2}{r}\cos^2\gamma - g\right) + \frac{D}{m}\sin\gamma - U\right] \tag{13}$$

For small bank-angle variations from the trimmed bank angle σ^* and small flight-path angles such that $\sigma = \sigma^* + \Delta\sigma$, the required control may be written using Eqs. (13) and (4) as

$$\Delta\sigma \cong \frac{m}{L\sin\sigma^*}\left(\frac{D}{m}\gamma - U\right) \tag{14}$$

which is singular for $\sigma^* = \pi$, since in this configuration there is no excess lift to exert control over the vehicle. This of course implies that the trimmed bank angle needs to be somewhat less than π.

Numerical Simulation

In order to validate the properties of the guidance scheme, a simple, low-fidelity numerical simulation was used with a waverider vehicle with m/C_LA of 50 kg · m^{-2} and lift-to-drag ratio of 10.[1] At an initial velocity of 15 km · s^{-1} and an altitude of 75 km in the Earth's atmosphere, the required equilibrium bank angle is 62 deg (zero bank angle in an inverted configuration). With a 1% perturbation to the initial altitude the vehicle rapidly climbs and prematurely exits the atmosphere via the instability mechanism previously described, Fig. 2a.

However, for a perturbation below the nominal trajectory it can be seen that the vehicle undergoes an inflection in altitude. This is not in fact a skip in the lower atmosphere, but is a hypersonic inverted loop, as demonstrated by a 360 deg rotation in the flight-path angle. Of course, the vehicle is found to experience unsustainable dynamic pressures.

Using the feedback linearization technique with $\lambda_1 = 0.01$ and $\lambda_2 = 0.1$, it is found that the initial perturbation is rapidly damped. The bank angle falls as low as 45 deg to generate sufficient control authority over the vehicle (Fig. 2b). For smallertrimmed bank angles the control quickly saturates and the vehicle is lost. A roll-rate limiter was not included in the simulation, so that rapid changes in commanded bank angle are seen to occur.

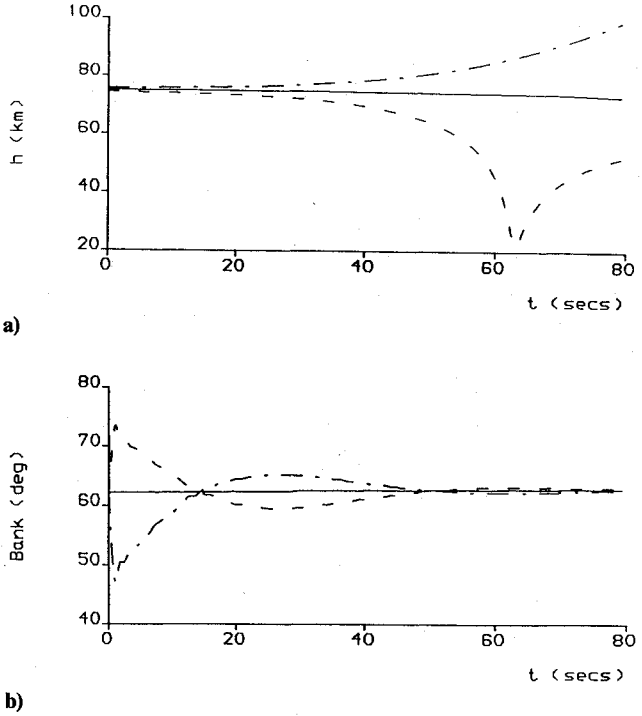

Fig. 2 a) Altitude time histories and b) bank-angle time histories (——— nominal trajectory; _ _ _ _ +1 % perturbation; - - - - - - -1% perturbation).

Conclusions

In this study it has been demonstrated that the AGA maneuver is dynamically unstable with respect to altitude errors. However, it has been shown that the instability may be controlled using feedback linearization. The existence of the instability further emphasizes the need for robust guidance during the atmospheric pass. Other related dynamical issues will be investigated in future studies.

References

[1]McRonald, A. D., and Randolph, J. E., "Hypersonic Maneuvring for Augmenting Planetary Gravity Assist," *Journal of Spacecraft and Rockets*, Vol. 29, No. 2, 1992, pp. 216–222.

[2]Randolph, J. E., and McRonald, A. D., "Solar System Fast Mission Trajectories Using Aerogravity Assist," *Journal of Spacecraft and Rockets*, Vol. 29, No. 2, 1992, pp. 223–232.

[3]Nonweiler, T. R. F., "Aerodynamic Problems of Space Vehicles," *Journal of the Royal Aeronautical Society*, Vol. 63, Sept. 1959, pp. 521–528.

[4]Van Buren, M. A., and Mease, K. D., "Aerospace Plane Guidance Using Time-Scale Decomposition and Feedback Linearization," *Journal of Guidance, Control, and Dynamics*, Vol. 2, No. 5, 1992, pp. 1829–1838.

Supersonic Axisymmetric Conical Flow Solutions for Different Ratios of Specific Heats

Bhavesh B. Patel,* B. K. Hodge,† and Keith Koenig‡
Mississippi State University,
Mississippi State, Mississippi 39762

Nomenclature

c_p = specific heat at constant pressure
c_v = specific heat at constant volume
h_o = stagnation enthalpy
M = Mach number
V_r' = dimensionless radial velocity, $V_r/V_{\max}$
V_θ' = dimensionless tangential velocity, $V_\theta/V_{\max}$
$V_{\max}$ = reference velocity, $\sqrt{2h_o}$
γ = ratio of specific heats, c_p/c_v
θ = polar coordinate in Eq. (1) or conical shock wave angle, deg
σ = cone semivertex angle, deg

Introduction

A NUMBER of sources[1,2] contain tabulations and charts for many useful compressible flow situations. For example, Refs. 1 and 2 both provide charts for conical supersonic flow of a calorically perfect gas over axisymmetric sharp cones with attached conical shock waves for a single ratio of specific heats, $\gamma = c_p/c_v = 1.405$ for Ref. 1 and $\gamma = 1.4$ for Ref. 2. Each contains sequences of charts with shock-wave angle, cone surface pressure coefficient, and cone surface Mach number vs cone semivertex angle, parameterized with freestream Mach number. No complementary study of conical flow has been reported for a variety of values of the ratio of specific heats.

Conical flows with different values of the ratio of specific heats are of interest because different gases have different specific heats ratios. Monatomic gases, such as helium, possess the largest value of γ, 1.67; diatomic gases, such as nitrogen and oxygen, and mixtures of diatomic gases, such as air, possess a ratio of specific heats of 1.4. The smallest value of γ is near unity for gases composed of very complex molecules. The value of $\gamma = 1.000001$ (hereinafter written as 1.0^+) represents the lower limiting case considered in this Note and is presented for completeness and as a demonstration of the robustness of the numerical technique.

The purpose of this Note is to summarize salient behavioral characteristics of calorically perfect conical supersonic flows for different values of the ratio of specific heats. A complete set of charts following the format of Ref. 1 is available in Patel et al.[3] Although the computation of such conical flows is relatively straightforward, some effort is required to assemble a useful set of information for a variety of values of γ. Over the possible range of the ratio of specific heats, $1.0^+ < \gamma < 1.67$, the characteristics show considerable variations.

Conical Supersonic Flow

A schematic of conical supersonic flow is presented in Fig. 1. A supersonic conical flowfield is defined by the following: 1) the shock wave is attached to the vertex of the cone, 2) the shock wave is conical in shape, 3) all flow properties are constant along radial lines, and 4) the flow between the shock wave and the cone surface is isentropic. The oblique shock relations hold across the conical shock wave. Conical supersonic flows were first solved graphically by Busemann[4] in 1929. In 1933, Taylor and Maccoll[5] derived the usually accepted conical flow equation,

$$\frac{\gamma-1}{2}\left[1-V_r'^2-\left(\frac{dV_r'}{d\theta}\right)^2\right]\left[2V_r'+\frac{dV_r'}{d\theta}\cot\theta+\frac{d^2V_r'}{d\theta^2}\right]-\frac{dV_r'}{d\theta}\left[V_r'\frac{dV_r'}{d\theta}+\frac{dV_r'}{d\theta}\frac{d^2V_r'}{d\theta^2}\right]=0 \quad (1)$$

and solved it numerically. Indeed, Anderson[6] views their paper and their numerical solution of Eq. (1), the Taylor-Maccoll equation, as a seminal point in the history of compressible flow. One of the first reported uses of digital computers in aerodynamics was the conical supersonic solutions of Kopal[7] that formed the basis of the charts in Ref. 1. Even after Kopal's report and the charts in Ref. 1, interest continued in such flows, and details of the flowfield about cones in supersonic flow were later tabulated by Sims.[8] Brower[2] provides additional historical details of the genesis of supersonic conical flow solutions.

The Taylor-Maccoll equation is an ordinary, nonlinear, second-order differential equation. The complexity of the differential equation precludes a closed-form solution. The results in this Note were

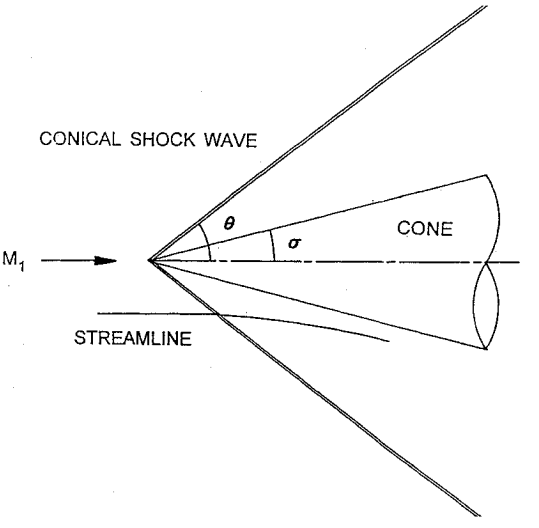

Fig. 1 Supersonic conical flow schematic.

Received June 18, 1993; revision received Sept. 7, 1993; accepted for publication Sept. 7, 1993.

*Undergraduate, Department of Aerospace Engineering; currently Graduate Research Assistant. Student Member AIAA.

†Professor, Department of Mechanical Engineering. Associate Fellow AIAA.

‡Professor, Department of Aerospace Engineering. Member AIAA.